



Scalable fabrication of stretchable and washable textile triboelectric nanogenerators as constant power sources for wearable electronics

Fan Xu^{a,c,1}, Shanshan Dong^{b,1}, Guoxu Liu^{a,c,1}, Chongxiang Pan^d, Zi Hao Guo^{a,c},
Wenbin Guo^{a,c}, Longwei Li^{a,c}, Yanping Liu^{b,*}, Chi Zhang^{a,c,d,**}, Xiong Pu^{a,c,d,**},
Zhong Lin Wang^{a,c,e}

^a CAS Center for Excellence in Nanoscience, Beijing Key Laboratory of Micro-nano Energy and Sensor, Beijing Institute of Nanoenergy and Nanosystems, Chinese Academy of Sciences, Beijing 101400, China

^b Engineering Research Center of Technical Textile of Ministry of Education, College of Textiles, Donghua University, Shanghai 201620, China

^c School of Nanoscience and Technology, University of Chinese Academy of Sciences, Beijing 100049, China

^d Center on Nanoenergy Research, School of Chemistry and Chemical Engineering, School of Physical Science and Technology, Guangxi University, Nanning, Guangxi 530004, China

^e School of Materials Science and Engineering, Georgia Institute of Technology, Atlanta, Georgia 30332-0245, USA

ARTICLE INFO

Keywords:

Triboelectric nanogenerators
Wearable electronics
Self-powered
Smart textile

ABSTRACT

The textile-based triboelectric nanogenerator (tTENG) is one of the most promising energy harvesting devices for realizing self-powered smart textiles and wearable electronics. Herein, we report a scalable machine-knitting fabrication of stretchable, washable and breathable tTENGs for harvesting human motion energies. A plating stitch technique is employed to fabricate tTENGs using various common yarn materials and working in different modes (coplanar sliding mode and contact-separation mode). The tTENG can output voltage up to 232 V and power density up to 66.13 mW/m². Furthermore, it can constantly power different wearable electronics by integrating with a small-size power management module, which converts the irregular AC output to a stable DC output and improves the energy utilization of tTENG. The stretchability, washability and air permeability of the tTENG are also demonstrated. These findings provide a practically viable textile-based power source that holds great promise in future self-powered wearable electronics and smart textiles.

1. Introduction

Wearable electronics have been receiving extensive attention as smart terminals for communication, entertainment, healthcare/sports care, human-machine interfaces, and so on [1–4]. Smart electronic textiles (E-textiles) are believed to be highly promising for next-generation wearable devices, considering their potentially better convenience and comfortability [5–8]. A variety of electronics have been realized in the form of fibers [9,10], yarns [11] or fabrics [12–14], and several types of E-textiles have emerged in the market, such as the heating suit and heart-rate suit. Nevertheless, one of the core challenges is to develop electric power textiles that could be breathable, washable, compatible with the traditional textile-manufacturing techniques, and

capable of withstanding complex deformations such as stretching, torsion and bending.

The textile-based triboelectric nanogenerator (TENG) is a promising candidate for the power device of E-textile [15–19]. The TENG can convert various mechanical energies into electricity through the coupled effects of contact electrification and electrostatic induction [20–22]. The two advantageous characteristics of the TENG, i.e. the vast materials choice and the high output for mechanical motions at low frequency, have made it an ideal choice for textile power devices [23–25]. Therefore, a variety of textile-based TENGs (tTENGs) have been reported with different fabric materials and textile structures to convert human motion kinetic energies into electricity [26–28]. However, the following issues are still required to address. Firstly, most studies have used coating [9,

* Corresponding author.

** Corresponding authors at: CAS Center for Excellence in Nanoscience, Beijing Key Laboratory of Micro-nano Energy and Sensor, Beijing Institute of Nanoenergy and Nanosystems, Chinese Academy of Sciences, Beijing 101400, China.

E-mail addresses: liuyup@dhru.edu.cn (Y. Liu), zhangchi@binn.cas.cn (C. Zhang), puxiong@binn.cas.cn (X. Pu).

¹ These authors contributed equally to this work.

29,30], electrospinning [31–33], dyeing [34] and other methods to attach conductive materials such as conductive polymers, metals and their derivatives, and carbon nanomaterials to the surface of the yarn [7]. Since the textile has variable bending structure, uneven surface morphology and complex material properties, the coatings covered on t-TENG are easy to peel off and have poor durability. In addition, it will reduce the flexibility, breathability of the tTENG, and comfort is far from ordinary fabrics. More importantly, the complex preparation process requires a lot of labor costs, making it difficult to achieve mass production. Though several works have reported tTENGs prepared using knitting or weaving techniques [6,35–37], it still requires further explorations to achieve simultaneously the combined properties of stretchability, washability, breathability, comfort, and scalable preparation. Secondly, considering the AC output characteristics of high voltage, high internal impedance and low current, the energy utilization of the tTENG is typically low when being employed directly as a power source for electronics [38,39]. Although several studies have improved the output voltage of tTENGs [13,40], power management circuits are still required to enlarge the effectively utilized energy in tTENG-based self-charging or self-powered systems [41–43]. Despite the recent progress on different conditioning circuits for TENGs, the applicability of these circuits on tTENGs has not been well studied yet.

Therefore, in this work, we propose a stretchable, washable, breathable and scalable machine-knitted tTENG, which is further demonstrated to be capable of providing constant power supplies for electronics by integrating with a small-size power management module (PMM). The tTENG is knitted with a plating stitch method, with the conductive yarn and dielectric yarn forming a knitting loop together but

at the top and down surfaces of the final textile, respectively. The softness of this double-faced tTENG, evaluated with a standard method, is comparable with commercial polyester fabrics. Both sliding-mode and contact-separation-mode tTENGs are demonstrated with high output performances (up to 232 V and 66.13 mW/m²). Even under low frequency, the tTENG in contact-separation mode still has a high output performance (128 V and 2.03 μ A at 1 Hz). This unique structure also makes the tTENG able to withstand various deformations like stretching, twisting and folding; meanwhile, it can be directly washed by the household laundry machine without a significant impact on its performances. Furthermore, we integrate the tTENG with a power management module (PMM) to reduce the voltage and improve the energy utilization, which makes the transferred charge and stored energy in a 15 mF capacitor 4 times and 16 times higher than that without the PMM, respectively. It is then demonstrated that the tTENG can provide a constant power supply for wearable electronics. Our work presents feasible and practical power alternatives for wearable electronics and E-textiles.

2. Results and discussion

2.1. The fabrication of tTENG

The tTENG was prepared by the plating stitch technique, so as to achieve a double-faced structure. One of the surfaces consists of dielectric yarns which function as an electrification layer to generate electrostatic charges; the other surface is made of conductive yarns which can output the inductive charges into the external circuits. This

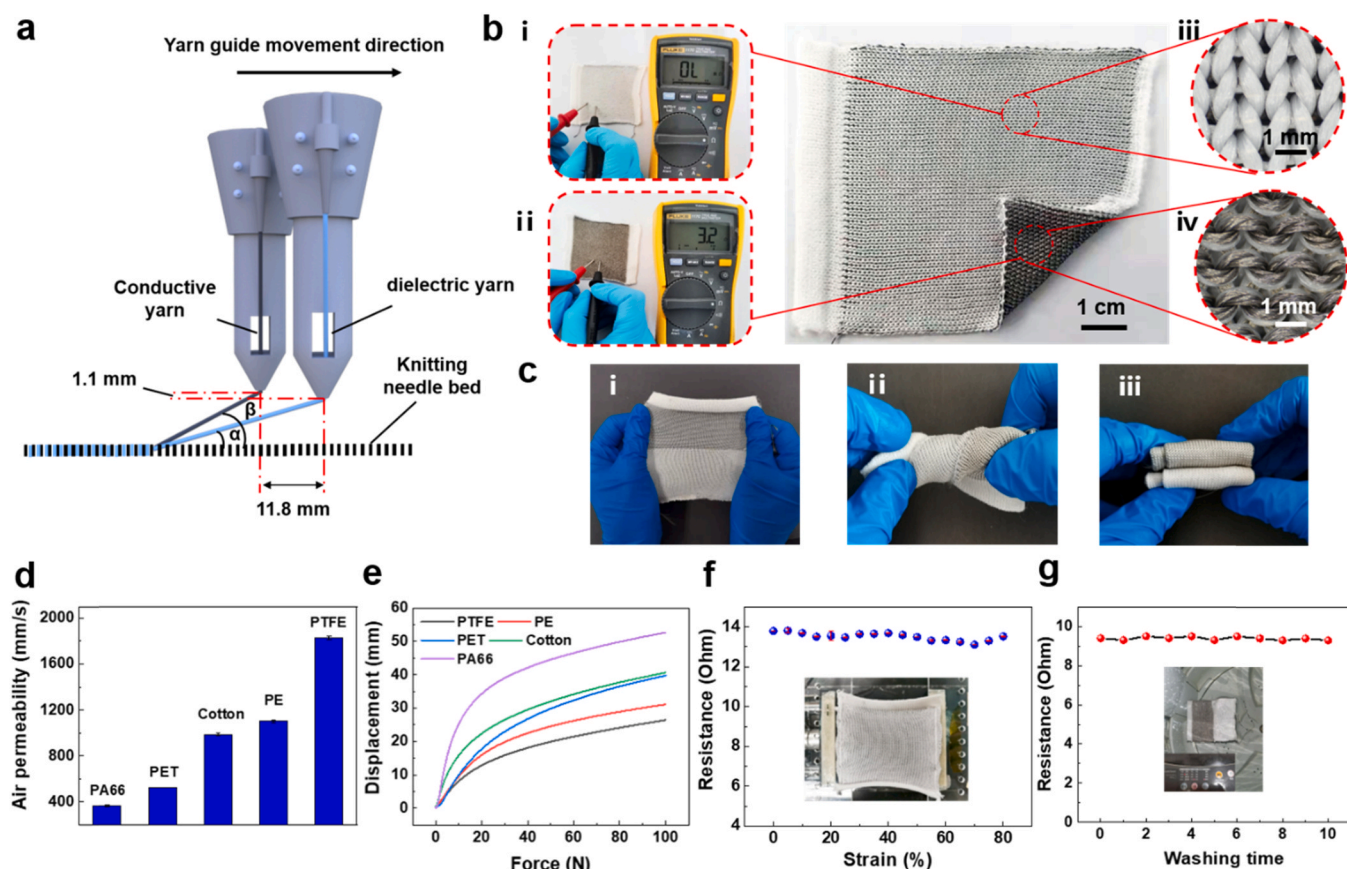


Fig. 1. Fabrication of the textile triboelectric nanogenerator (tTENG). (a) The schematic illustration of the fabrication process of the tTENG using a plating stitch technique. (b) The photographs of a tTENG with double-faced structure: upside surface consisting of insulating dielectric yarns (i, iii), and downside surface consisting of conductive yarns (ii, iv). (c) The photographs demonstrating that the tTENG is deformable. (d) The air permeability and (e) displacement-force curve of tTENGs with different dielectric yarns. (f) Variation in resistance of electrode layer of a tTENG under different tensile strains. The inset photograph shows a tTENG under 50% strain. (g) Variation in resistance of electrode layer of a tTENG after washing for different times. The inset photograph is a tTENG in a laundry machine.

structure is analogous to the stacked thin films, but characteristics of fabrics are remained, such as breathability and stretchability. Fig. 1a illustrates the principle of the plating stitch technique. The conductive yarn and dielectric yarn are fed into the knitting needles at the same time. The conductive yarn guide is located behind the dielectric yarn guide, and the conductive yarn feeder is 11.8 mm horizontally apart from the dielectric yarn feeder and 1.1 mm vertically. During the knitting process, the longitudinal angle α of the dielectric yarn is always smaller than the longitudinal angle β of the conductive yarn. When the knitting needle descends and hooks the two yarns to form a loop, the dielectric yarn is always right underneath the conductive yarn. After all loops being tightly knitted together, dielectric yarns are only exposed to one surface and conductive yarns are exposed to the other. In our study, commercial Ag-coated nylon yarns were chosen as the conductive yarns, considering their combined advantages of high conductivity, softness, and mechanical robustness. The resistance of a 1 cm long Ag-coated nylon yarn only increased from 3.06 Ohm to 14.18 Ohm after harsh abrasion with another PA66 fabric 6000 times (Fig. S1a). No significant peeling off of the Ag coatings was observed under scanning electron microscopy (SEM) as well (Fig. S1b–c). Dielectric layer is made of a series of different dielectric yarns, including polytetrafluoroethylene (PTFE) filament, polyamide (PA66) multifilament, polyethylene (PE) filament, polyethylene terephthalate (PET) and cotton yarns. Loops of insulating dielectric yarns and Ag yarns were nested with each other to form a plating stitch with a stable structure. As shown in Fig. 1b, the upside surface of a tTENG is made of dielectric yarns to form the triboelectric layer, and the downside is made of Ag yarns to form the electrode layer. The upside surface is insulating (Fig. 1b<i>>) and the lower downside surface is highly conductive (Fig. 1b<ii>), due to the fact that the yarns are knitted densely together and no conductive yarns are exposed to the top surface (Fig. 1b<iii>, iv>).

To demonstrate the flexibility of tTENG, the photographs of tTENG at stretched, twisted and folded states are displayed in Fig. 1c. The air permeability of double-faced tTENG fabrics prepared with different dielectric yarns was tested according to national standard of GB/T 5453-1997. As shown in Fig. 1d, the tTENG fabricated with PTFE filaments shows the highest air permeability of 1826.4 mm/s; while the air permeability of tTENG using highly elastic PA66 is the lowest (364.8 mm/s), which is still comparable to most ordinary clothing fabrics. These results demonstrate that the tTENGs have outstanding breathability. The stretchability of these fabrics were also examined, as shown by the displacement-force profiles in Fig. 1e. When applying a force of 100 N to tTENGs, all the tested fabrics can be stretched, among which the tTENG with PA66 multifilaments showed the highest displacement of 52 mm (correspondent to 81% tensile strain). The resilience of the tTENG was also evaluated by tensile loading-unloading tests (Fig. S2), confirming the tTENG is elastic and the stretch strain can be recovered. Furthermore, the resistance of the fabric electrodes at stretched states showed very little variation at the stretching strains up to 80% (Fig. 1f). A tTENG was also washed with a home laundry machine 10 times (800 rpm, 7 min for each time), no degradation of the electrodes was observed (Fig. 1g).

The basic parameters of tTENGs knitted with different yarn materials are shown in Table 1. The thickness of double-faced tTENGs is similar to normal knitted air layer fabrics, which have been widely used in

hoodies. The stitch density and specific areal weight of these tTENG fabrics suggesting their lightweight and softness. The softness of the tTENG was further tested by Kawabata Evaluation System. Bending stiffness and bending hysteresis are indicators of fabric bending performance, which directly indicate the softness of the fabric. The smaller the bending stiffness value, the easier it is for the fabric to be bent. The smaller the bending hysteresis, the better the bending recovery of the fabric. The bending stiffness and bending hysteresis of PA66 are 0.0570 and 0.1171, respectively. These are closed to the common polyester fabrics, whose bending stiffness and bending hysteresis are 0.063 and 0.026, respectively. Therefore, the tTENG has excellent stretchability, breathability, washability, and comfortability. Considering that all the yarn materials can be easily accessed and the fabrics are machine-knitted, the fabrication is also scalable.

2.2. The coplanar tTENG working at sliding mode

We first prepared a tTENG with a coplanar structure working at the sliding mode for harvesting human kinetic mechanical energy. As schematically shown in Fig. 2a, the two coplanar electrodes were knitted underneath PE and PA66 yarns, respectively. PA66 and PE were selected by both considering their close thickness and large difference in the triboelectric series table. To ensure that the two electrodes are not shorted, no Ag yarn was added at the junction of the two fabrics, but only PA66 and PE yarns were connected. As the PA66 and PE vary significantly in the triboelectric series table, the polarity or quantity of the electrostatic charges in these two yarns will be different. For example, if another PA66 textile is rubbing on the coplanar tTENG (Fig. 2b), negative static charges will be generated in the PE yarns, while the quantity of static charges in the other part of PA66 will be little (Fig. 2b stage i). When the top PA66 textile slides from the underneath PE side to the PA66 side, there would be an inductive current flowing from the electrode on the left-hand side to the right-hand side through the external circuit, so as to achieve the local charge equilibrium (Fig. 2b stage ii). The current flux will be stopped when all the static charges are screened (Fig. 2b stage iii), but the current in the reverse direction will be generated again when the top PA66 textile slides back (Fig. 2b stage iv). In this way, the repeated reciprocating rubbing motions of the fabrics will be converted to AC current.

For selecting a suitable material for the rubbing textile, five common fabrics were tested using a linear motor at a motion frequency of 3 Hz. For all tests, the top rubbing textile is about $4 \times 8.5 \text{ cm}^2$, and the underneath double-faced coplanar textile is about $8 \times 8 \text{ cm}^2$. The results showed that when another PA66 is used as the rubbing textile, the output performance of is the highest (Fig. S3), achieving a voltage of 120 V and a current of about 1.6 μA . The maximum power density is 5.58 mW/m^2 at an external resistance of 70 MOhm (Fig. 2e). Owing to its high performance, it can light up 200 LEDs easily, as shown in the inset in Fig. 2e. The frequency-dependent electrical output performances of the tTENG are shown in Fig. S4, exhibiting that the voltage and current increase as the frequency increases from 1 to 5 Hz, but transferred charge keeps relatively stable. The output voltage and current of tTENG are higher than several other researches because the fabric prepared by the plating stitch technique is more delicate, which may increase the effective contact area between the fabrics [6,35].

Table 1
The basic parameters of tTENGs knitted with different yarn materials.

Material	Size (cm^2)	Lateral stitch density ($(5 \text{ cm})^{-1}$)	Vertical density ($(5 \text{ cm})^{-1}$)	Mass (g m^{-2})	Thickness (mm)	Bending stiffness ($\text{gf.cm}^2/\text{cm}$)	Bending hysteresis (gf.cm/cm)
PTFE	6.5×6.5	37	49	672.07	0.825	0.1212	0.1669
PA66	6.5×5.7	37	56	352.63	0.9	0.0570	0.1171
PE	6.8×7.0	36	46	360.21	0.895	0.1325	0.1242
PET	6.6×5.7	37	56	379.74	1.04	0.2164	0.3908
Cotton	6.5×5.9	38	50	379.47	0.925	0.0626	0.0717

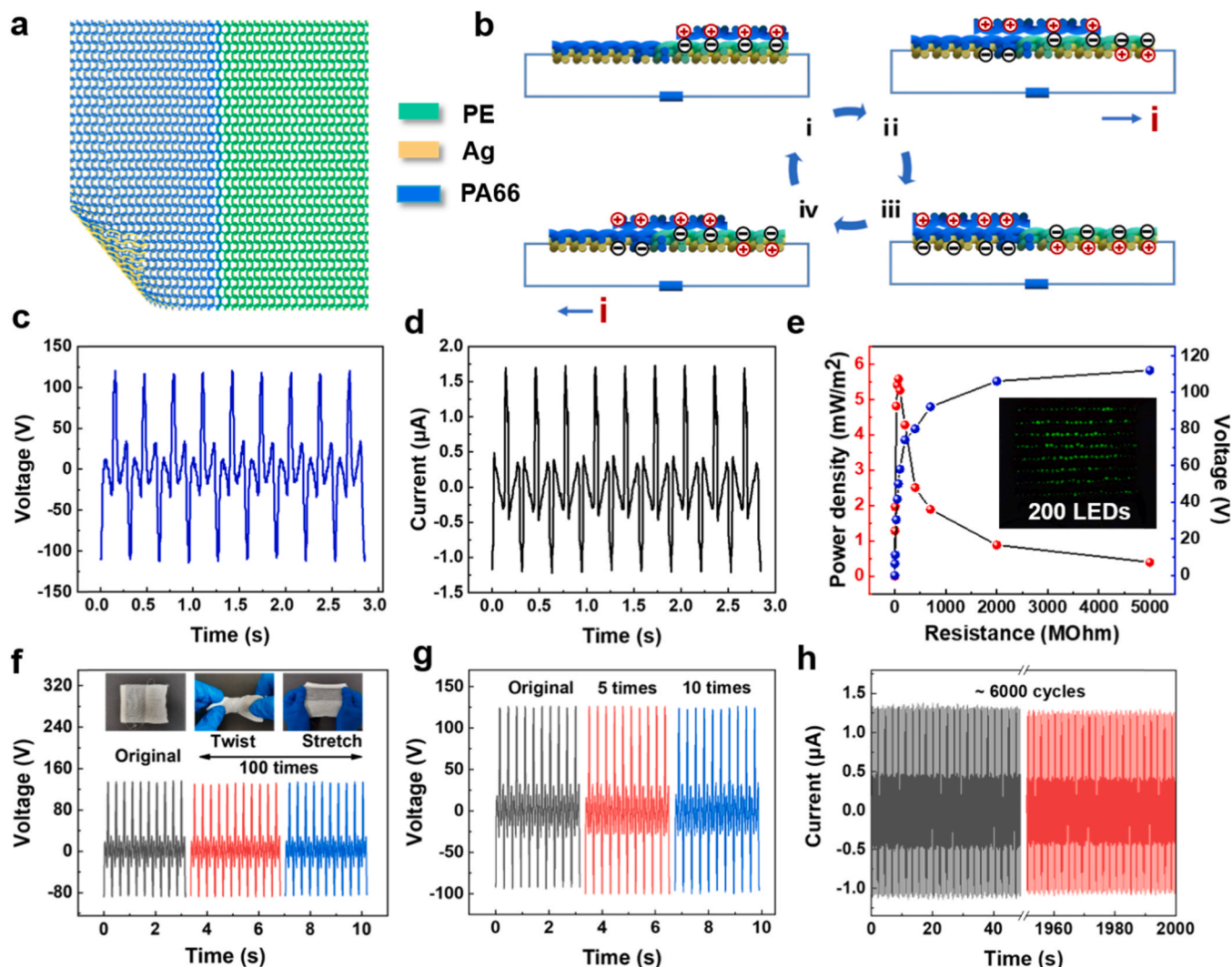


Fig. 2. Output performances of a tTENG in coplanar sliding mode. (a) Schematic illustration of the tTENG. (b) Working mechanism of the tTENG. (c) The output open-circuit voltage and (d) short-circuit current of the tTENG (area: $8 \times 8 \text{ cm}^2$, frequency: 3 Hz). (e) The output power density and voltage with different external load resistances. The inset photograph shows that 200 LEDs were lit by the tTENG. (f) The output voltage of the tTENG after suffering various deformations. (g) The output voltage of the tTENG after washing for 10 times. (h) The current of the tTENG before and after 6000 cycles of sliding motions.

Considering the request for comfort and convenience of textile power devices, flexibility, washability and durability are all critical properties. As shown in Fig. 2f, the output voltage of the tTENG did not change obviously, after twisting and stretching 100 times respectively. Then, the tTENG was directly washed by a household washing machine without packaging, and it was demonstrated the process of multiple violent washing and drying has no effect on tTENG output (Fig. 2g). In addition, the result shows that the voltage has no significant decrease during 6000 cycles of rubbing test (Fig. 2h), suggesting that the tTENG exhibits good mechanical robustness and working durability. The excellent flexibility, washability and durability of tTENG are because that its electrode yarns and electrification yarns are not simply attached, but are nested together tightly with knitting loops. In addition, there is no chemical coating on the surface of the insulating yarn and the conductive yarn, so external stimuli will not affect the stability of their structure and electrical properties.

2.3. The tTENG working at vertical contact-separation mode

With the plating stitch technique, the tTENG working at vertical contact-separation mode can be realized easily, which only requires two double-faced textiles with different top insulating yarns, as shown in

Fig. 3a. PA66 yarns and PTFE yarns were selected as the two dielectric yarns, since the PA66 is one of the most tribo-positive materials and PTFE is among the most tribo-negative materials. When the PTFE yarn is in contact with the PA66 yarn, static charges with different polarities will be generated in these two yarns (Fig. 3b, stage i). When they are separated from each other, positive charges will be induced in the electrode at the backside of PTFE, and negative charges will be induced in the electrodes at the backside of PA66 for charge equilibrium, yielding a current flowing from the electrode underneath PA66 to that underneath PTFE (Fig. 3b, ii). The current stops when static charges are all balanced by inductive charges (Fig. 3b, iii), and flows in reverse direction again when the two textiles approach back into contact (Fig. 3b, iv). We prepared a tTENG with an effective contact area of $6.5 \times 6.5 \text{ cm}^2$. 30 mm separation distance was fixed for all tests (Fig. S5). When the contact separation motion is at about 3 Hz frequency, the voltage reaches a value of 232 V (Fig. 3c) and the current is $6.8 \mu\text{A}$ (Fig. 3d). The maximum power density reaches 66.13 mW/m^2 at the external load of 10 MOhm (Fig. 3e). The tTENG can also light up 250 LEDs easily due to its high output performance (inset in Fig. 3e). The high voltage is also attributed to the delicate and tight knitting surface. Meantime, the tightly knitted structure between the top insulating and underneath conductive yarns is also beneficial for the generation of

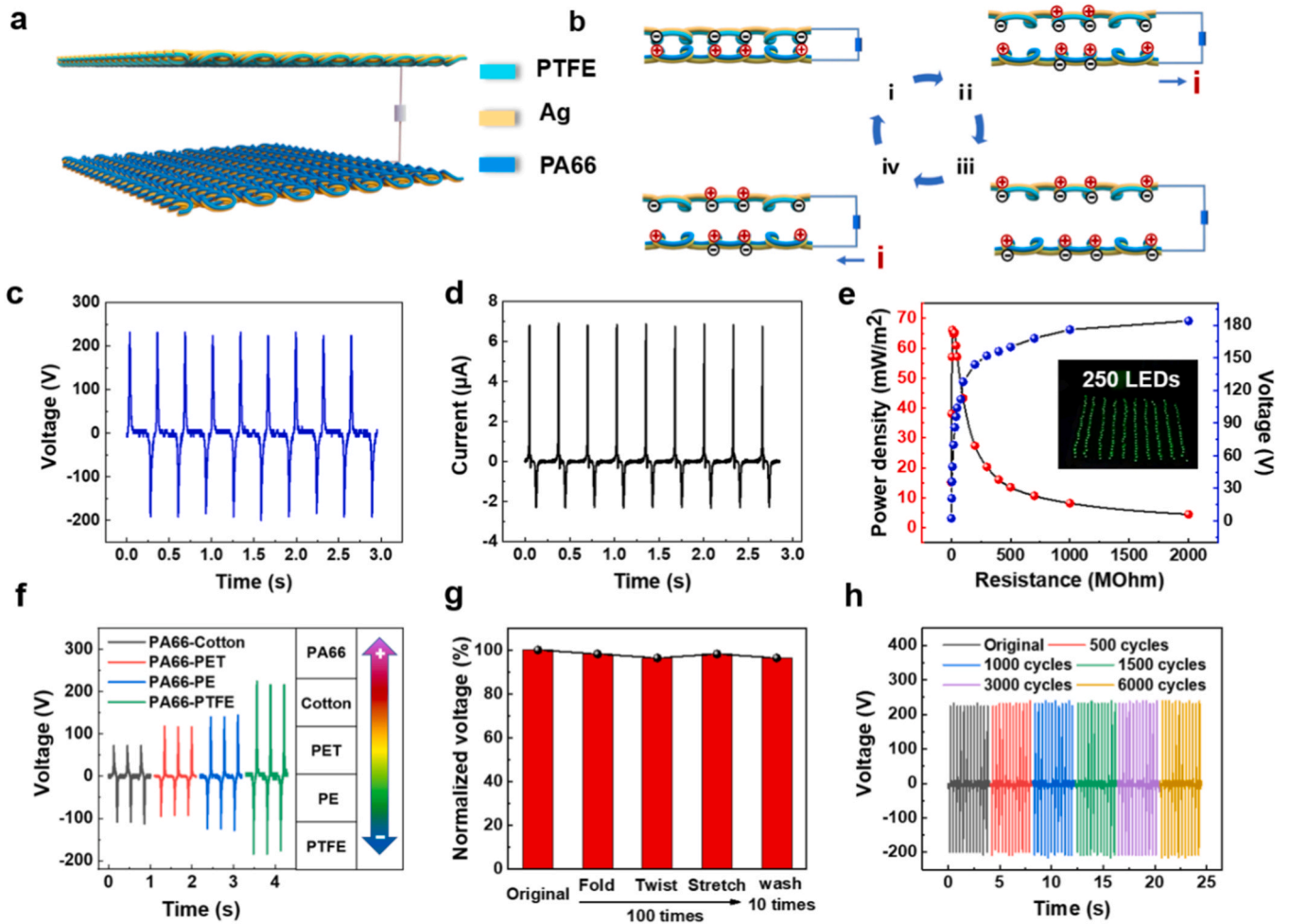


Fig. 3. Output performances of a tTENG in contact-separation mode. (a) Schematic illustration of the tTENG. (b) Working mechanism of the tTENG. (c) Output open-circuit voltage and (d) short-circuit current of the tTENG at a motion frequency of 3 Hz. (e) The output power density and voltage of tTENG with different external load resistances. The inset photograph shows that 250 LEDs were lit by the tTENG. (f) Output voltage of the tTENG using different pairs of triboelectric yarn materials and the corresponding triboelectric series. (g) Normalized voltage of the tTENG after various mechanical demonstration and washing by laundry machine. (h) The voltage of the tTENG before and after 6000 cycles of contact-separation motions.

inductive charges.

We also prepared the tTENG using different insulating yarns, as shown by the corresponding photos in Fig. S6. Their output voltages are compared in Fig. 3f, where the tTENG using PA66 and PTFE as the contact-separation pairs shows the highest voltage. This is accordant with the triboelectric series table, that the larger difference in the triboelectric series of the electrification pairs leads to the higher output of the tTENG. Fig. S7 shows the voltage and current increase as the frequency increases from 1 to 5 Hz, but transferred charge keeps relatively stable. The same variation trend of the current and voltage is because that the voltage was measured by an oscilloscope with an internal resistance of only 100 MOhm. In addition, under low frequency, the tTENG still has a high output performance. The outputs under 1 Hz can still reach 128 V, 51.29 nC, 2.03 μ A. For 5 Hz contact-separation motion, the voltage reaches 344 V and the current reaches 12.92 μ A. The capability of the tTENG to withstand various deformation and machine washing was also examined, that no degradation is observed after 100 times of folding, twisting, stretching, and 10 times of washing by a household laundry machine (Fig. 3g). The long-term durability was confirmed by the fact that there is no degradation of the output throughout 6000 cycles of contact-separation motions (Fig. 3h).

2.4. The power management module (PMM)

As discussed above, the tTENG has pulsed AC outputs with high voltage and low current, which have to be managed with conditioning circuits for a stable power supply to the electronics. The management circuits should have the following functions, *i.e.* AC-DC conversion, voltage step-down, and a hysteresis switch to maximize the output U - Q plot area of the TENG. The power management module (PMM) (Fig. 4a) consists of a bridge rectifier for AC-DC conversion, a DC-DC buck converter (parallel diode D , series inductor L , and parallel capacitor C) for voltage step-down conversion, and a hysteresis switch which is automatically controlled based on the voltage of the TENG by a metal-oxide-semiconductor field-effect transistor (MOSFET) and a comparator, the inductor (L) has an inductance of 5 mH, and the capacitance of the capacitor (C) is 14 μ F. The LC unit forms a low-pass filter, which can restrain the high-frequency harmonic component in output voltage, so a stable and constant DC output voltage will be generated across the load. The DC voltage on a series of different load resistors was recorded in Fig. 4b. The voltage rises rapidly with time at the beginning stage due to the charging of the capacitor and then remains stable. The saturated voltage increases with the increase of the resistance. The saturated DC voltage is about 2.3 V for a load resistance of 1 MOhm, and 17.9 V for the resistance of 3 GOhm.

To demonstrate the capability of the PMM in improving the energy

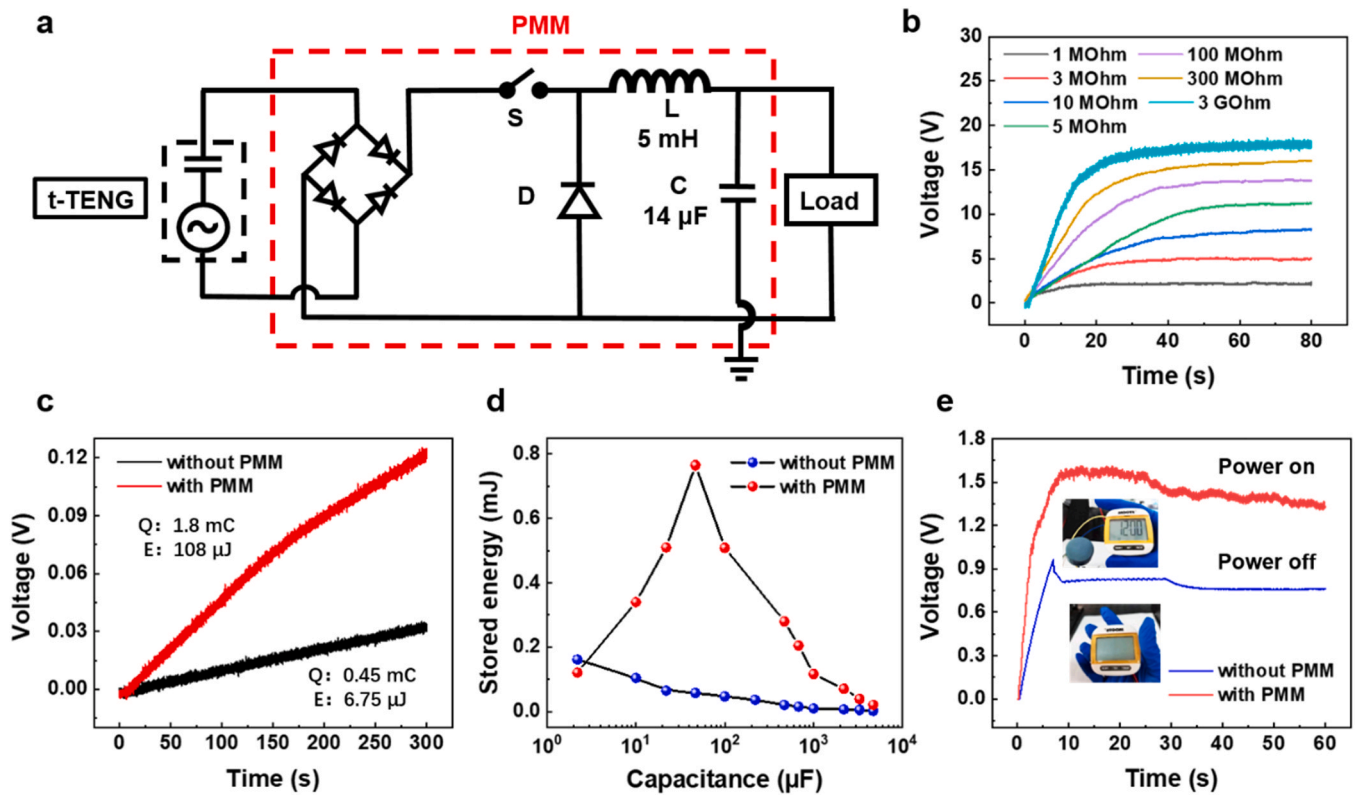


Fig. 4. Power management module (PMM). (a) The equivalent circuit of a power management module. (b) Voltage drop of external load resistors with different resistances, confirming the constant DC electricity converted by the PMM. (c) The voltage of a 15 mF capacitor charged by the tTENG with and without a PMM. (d) The stored energy of a series of capacitors (2.2 μF to 4700 μF) charged by the tTENG in 100 s with and without PMM. (e) The voltage profiles of a 14 μF capacitor when being connected to drive a pedometer. The tTENG was simultaneously charging the capacitor with and without the PMM.

utilization by the back-end load, a tTENG working at contact-separation mode with an area of $10 \times 10 \text{ cm}^2$ was utilized, which can output a voltage of 344 V and a current of 12.51 μA (Fig. S8). A 15 mF capacitor was connected as an external load to store the converted electricity. If without PMM, the capacitor was charged from 0 V to 0.03 V in 300 s; if there was a PMM, the voltage increased from 0 V to 0.12 V in the same time period (Fig. 4c). The stored charge quantity and energy with the PMM is 1.8 mC and 108 μJ , which is 4 times and 16 times higher than that without the PMM, respectively. A series of different capacitors (2.2 μF to 4700 μF) were then connected as the load and charged for the same time period (100 s). Without PMM, the highest stored energy of 0.16 mJ is obtained when the capacitor is 2.2 μF ; while with PMM, the highest stored energy of 0.76 mJ is obtained at an optimum capacitor of 47 μF (0.058 mJ without PMM), as shown in Fig. 4d. Therefore, it is clearly proved that the stored charge capacity and energy have been significantly improved by integrating with the PMM.

Wearable electronic devices were then powered by the tTENG integrated with the PMM. When a pedometer was connected to the PMM as a load, the voltage increased to 1.56 V in 8 s (Fig. 4e), and then the pedometer turned on automatically (the inset photo in Fig. 4e). Subsequently, the voltage maintained to be about 1.35 V after a slight decrease and the pedometer operate constantly for about 60 s, which means that energy consumption by the pedometer had been fully compensated by the tTENG and a self-powered wearable device was realized without extra power devices (see also Video S1). On the contrary, the tTENG, only with a bridge rectifier and 14 μF capacitor, could not turn the pedometer on automatically and power it constantly. The voltage was always below the threshold value to turn on the pedometer.

2.5. Self-powered wearable devices based on tTENGs

The tTENGs working at both the contact-separation mode and coplanar sliding mode were sewed on a sleeve of a common cloth to examine their performances in harvesting human kinetic energy and in serving as self-powered wearable devices (Fig. 5a). A tTENG at coplanar sliding mode ($8 \times 8 \text{ cm}^2$) was able to output voltage of 76 V and current of 0.86 μA when swinging one arm (Fig. S9). A tTENG at contact-separation mode ($10 \times 10 \text{ cm}^2$) could output voltage of 256 V (Fig. 5b) and current of 7.2 μA (Fig. S10) when swinging the arm. The PMM was packaged into a cylindrical shape with a diameter of 2 cm and height of 0.4 cm, which could be designed as a brooch or a button of a cloth considering its small size (Fig. 5a<ii>). Then, the whole self-powered system could be integrated into a power textile, which could harvest the human motion energy for a constant power supply to small electronics. As shown in the Video S2, an electronic watch and a calculator (see also Fig. 5a <iii-v>) can all be constantly powered by this power textile. Without the PMM, the tTENG fixed on a cloth can only power the electronic watch intermittently (about 55 s energy accumulation and 8 s operation), as shown in Fig. 5c; with the PMM, the electronic watch can be turned on automatically and operate constantly when swinging the arm (Fig. 5d). These results strongly support that the textile-based self-powered wearable devices have been successfully demonstrated with the tTENG. For electronics with low power consumption, this self-powered system enabled their constant operation without batteries or other energy devices. For the future studies, the performances of self-powered systems need to be further improved, so that a cloth could be a platform (Fig. 5a<vi>) which may be able to provide power supplies to various wearable devices, so as to realize the applications in smart care, virtual reality/augmented reality (VR/AR), smart homes, and so on [23].

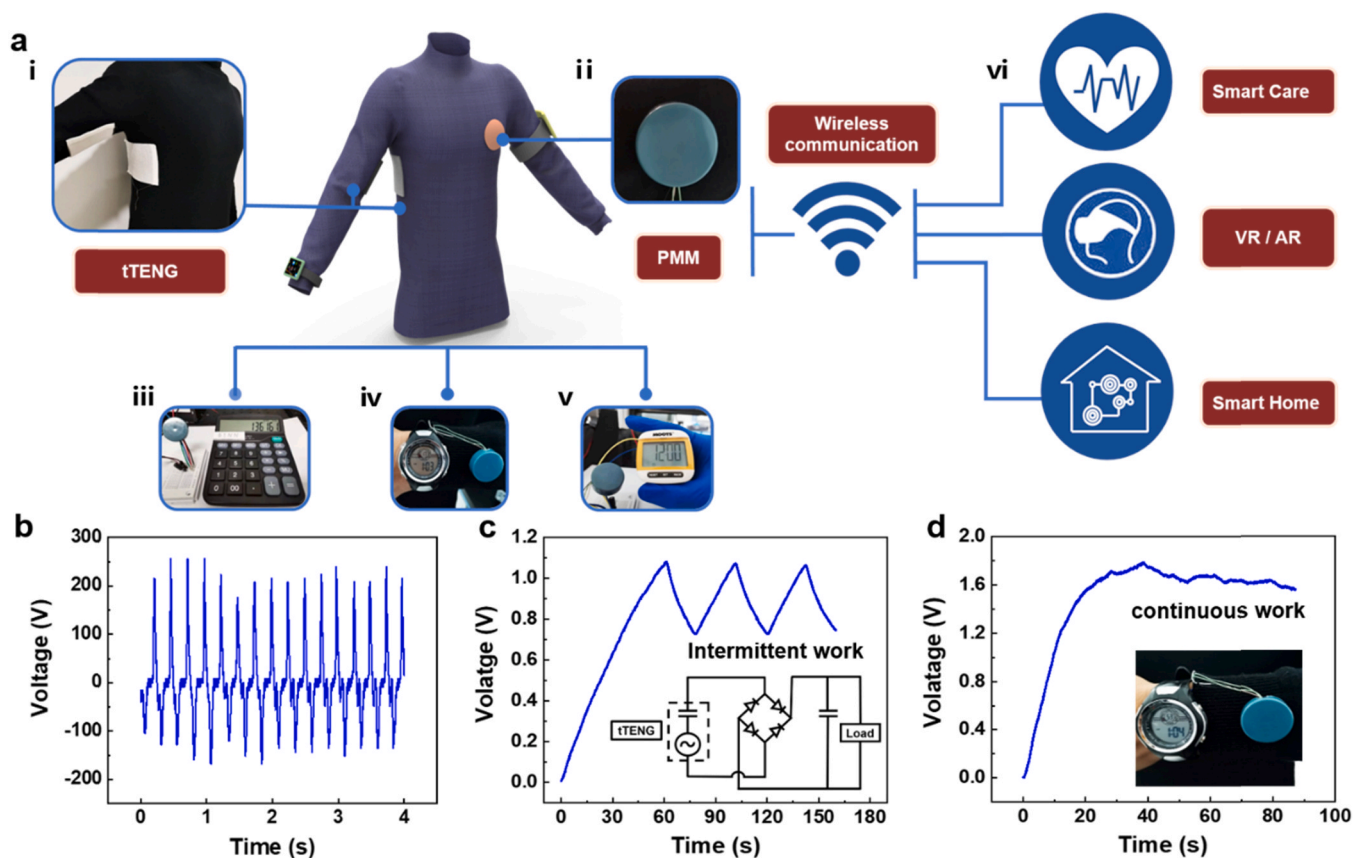


Fig. 5. Self-powered electronics driven by the tTENG. (a) The schematic illustration of various self-powered smart electronics driven by the tTENG. (i) the tTENG, (ii) the PMM, (iii-iv) photographs of electronics powered by the tTENG, and (vi) smart self-powered electronics for future explorations. (b) The voltage of a tTENG recorded when wearing it on a human body. (c) The intermittent operation and (d) constant operation of the electronic watch driven by the tTENG without PMM and with PMM, respectively, when wearing it on a human body.

Supplementary material related to this article can be found online at [doi:10.1016/j.nanoen.2021.106247](https://doi.org/10.1016/j.nanoen.2021.106247).

3. Conclusion

In summary, we achieved a machine knitted tTENG, which was stretchable, washable, breathable and facile for scalable production. The plating stitch technique made the tTENG able to be fabricated with various yarn materials and to operate at different working modes. The tTENG working at contact-separation mode and sliding mode was demonstrated, achieving high output up to 232 V and 66.13 mW/m². Furthermore, a small-sized PMM was designed to convert the irregular AC output of the tTENG into a stable DC electricity and improved the energy utilization, which was then employed to provide constant power supplies to several wearable electronic devices. These results suggested that this power textile could be potentially a platform for a variety of self-powered smart electronics.

4. Experimental section

4.1. Materials

PTFE filament (550 dtex) was bought from Suzhou Nett New Material Technology Co., Ltd., Suzhou, Jiangsu, China. PA66 multifilament (250 D) was bought from Xinxiang Rixin Ecological Textile Clothing Co., Ltd., Xinxiang, Henan, China. Ag-plated nylon6 multifilament (280 D) was bought from Qingdao Tianyin Textile Technology Co., Ltd., Qingdao, Shandong, China. Polyester multifilament (200 D) was bought from Tongxiang Tonglun Textile Co., Ltd., Tongxiang, Zhejiang, China.

Polyethylene multifilament (400 D) was bought from Honeywell Co., Ltd., Shanghai, China.

4.2. Fabrication of the tTENG

The machine knitted tTENG is fabricated by plating stitch technique through a computerized flat knitting machine (Stoll CMS ADF 530-32 W E7.2, KARL MAYER STOLL Textilmaschinenfabrik GmbH, Reutlingen, Germany). Dielectric yarns (PTFE filament, PA66 multifilament, polyester multifilament, PE filament, cotton yarns) and Ag yarns were used to knit into a plating stitch fabric. Two double-faced fabrics with different dielectric yarn materials were used for constructing vertical contact-separation-mode tTENGs. As for coplanar tTENG, PE filament and Ag yarns were first used to fabricate the PE part, then PA66 yarns were used with the Ag yarns to form the PA66 part. No Ag yarn was added at the junction of the two fabrics in order to avoid short circuit caused by the connection of the two electrodes.

4.3. Characterization

The enlarged surface of the fabric was captured with a stereo microscope (NIKON SMZ745T, China). The Kawabata Evaluation System was used to test the softness of the tTENG. A linear motor (LinMot E1200, USA) was applied to provide a periodic reciprocating movement of tTENG. An electrometer (Keithley 6517B, USA) was used to test the short-circuit current and transferred charge of the tTENG. A mixed domain oscilloscope (Tektronix MDO3024, USA) with a 100MΩ high voltage probe was used to test the open-circuit voltage of the tTENG. An automatic breathability tester (YG461H, China) was used to evaluate the

breathability of the tTENG, and an electronic fabric strength tester (YG028, China) was used to measure the stretchability of the tTENG.

CRedit authorship contribution statement

Fan Xu: Conceptualization, Methodology, Data curation, Investigation, Writing - original draft, Writing - review & editing. **Shanshan Dong:** Methodology, Data curation. **Guoxu Liu:** Data curation, Investigation, Writing - original draft. **Chongxiang Pan:** Data curation, Visualization. **Zi Hao Guo:** Methodology, Investigation. **Wenbin Guo:** Data curation, Investigation. **Longwei Li:** Visualization, Investigation. **Yanping Liu:** Supervision, Writing - review & editing. **Chi Zhang:** Supervision, Writing - review & editing. **Xiong Pu:** Supervision, Conceptualization, Writing - original draft, Writing - review & editing. **Zhong Lin Wang:** Supervision, Writing - review & editing.

Declaration of Competing Interest

The authors declare that they have no known competing financial interests or personal relationships that could have appeared to influence the work reported in this paper.

Acknowledgements

The authors thank for the support from National Key Research and Development Program of China (2016YFA0202702), Shanghai Pujiang Program (17PJ1400300), the Youth Innovation Promotion Association of Chinese Academy of Sciences.

Appendix A. Supporting information

Supplementary data associated with this article can be found in the online version at [doi:10.1016/j.nanoen.2021.106247](https://doi.org/10.1016/j.nanoen.2021.106247).

References

- [1] R. Hinchet, H.J. Yoon, H. Ryu, M.K. Kim, E.K. Choi, D.S. Kim, S.W. Kim, Transcutaneous ultrasound energy harvesting using capacitive triboelectric technology, *Science* 365 (2019) 491–494, <https://doi.org/10.1126/science.aan3997>.
- [2] G. Chen, Y. Li, M. Bick, J. Chen, Smart textiles for electricity generation, *Chem. Rev.* 120 (2020) 3668–3720, <https://doi.org/10.1021/acs.chemrev.9b00821>.
- [3] N.N. Zhang, Y.Z. Li, S.W. Xiang, W.W. Guo, H. Zhang, C.Y. Tao, S. Yang, X. Fan, Imperceptible sleep monitoring bedding for remote sleep healthcare and early disease diagnosis, *Nano Energy* 72 (2020), 104664, <https://doi.org/10.1016/j.nanoen.2020.104664>.
- [4] M.L. Zhu, Z.D. Sun, Z.X. Zhang, Q.F. Shi, T.Y.Y. He, H.C. Liu, T. Chen, C.K. Lee, Haptic-feedback smart glove as a creative human-machine interface (HMI) for virtual/augmented reality applications, *Sci. Adv.* 6 (2020) 8693, <https://advances.sciencemag.org/content/6/19/eaaz8693>.
- [5] J. Xiong, P.S. Lee, Progress on wearable triboelectric nanogenerators in shapes of fiber, yarn, and textile, *Sci. Technol. Adv. Mater.* 20 (2019) 837–857, <https://doi.org/10.1080/14686996.2019.1650396>.
- [6] S.S. Dong, F. Xu, Y.L. Sheng, Z.H. Guo, X. Pu, Y.P. Liu, Seamlessly knitted stretchable comfortable textile triboelectric nanogenerators for e-textile power sources, *Nano Energy* 78 (2020), 105327, <https://doi.org/10.1016/j.nanoen.2020.105327>.
- [7] K. Dong, X. Peng, Z.L. Wang, Fiber/fabric-based piezoelectric and triboelectric nanogenerators for flexible/stretchable and wearable electronics and artificial intelligence, *Adv. Mater.* 32 (2020), 1902549, <https://doi.org/10.1002/adma.201902549>.
- [8] X.P. Chen, X.K. Xie, Y.N. Liu, C. Zhao, M. Wen, Z. Wen, Advances in healthcare electronics enabled by triboelectric nanogenerators, *Adv. Funct. Mater.* 30 (2020), 2004673, <https://doi.org/10.1002/adfm.202004673>.
- [9] J.L. Chen, X.J. Wen, X. Liu, J.Q. Cao, Z.H. Ding, Z.Q. Du, Flexible hierarchical helical yarn with broad strain range for self-powered motion signal monitoring and human-machine interactive, *Nano Energy* 80 (2021), 105446, <https://doi.org/10.1016/j.nanoen.2020.105446>.
- [10] Q. Shi, J. Sun, C. Hou, Y. Li, Q. Zhang, H. Wang, Advanced functional fiber and smart textile, *Adv. Fiber Mater.* 1 (2019) 3–31, <https://doi.org/10.1007/s42765-019-0002-z>.
- [11] K. Dong, Z. Wu, J. Deng, A.C. Wang, H. Zou, C. Chen, D. Hu, B. Gu, B. Sun, Z. L. Wang, A stretchable yarn embedded triboelectric nanogenerator as electronic skin for biomechanical energy harvesting and multifunctional pressure sensing, *Adv. Mater.* 30 (2018), 1804944, <https://doi.org/10.1002/adma.201804944>.
- [12] C. Ye, Q. Xu, J. Ren, S. Ling, Violin string inspired core-sheath silk/steel yarns for wearable triboelectric nanogenerator applications, *Adv. Fiber Mater.* 2 (2020) 24–33, <https://doi.org/10.1007/s42765-019-00023-w>.
- [13] J. Xiong, P. Cui, X. Chen, J. Wang, K. Parida, M.F. Lin, P.S. Lee, Skin-touch-actuated textile-based triboelectric nanogenerator with black phosphorus for durable biomechanical energy harvesting, *Nat. Commun.* 9 (2018) 4280, <https://doi.org/10.1038/s41467-018-06759-0>.
- [14] K. Fu, Z. Yang, Y. Pei, Y. Wang, B. Xu, Y. Wang, B. Yang, L. Hu, Designing textile architectures for high energy-efficiency human body sweat- and cooling-management, *Adv. Fiber Mater.* 1 (2019) 61–70, <https://doi.org/10.1007/s42765-019-0003-y>.
- [15] H. Wang, M. Han, Y. Song, H. Zhang, Design, manufacturing and applications of wearable triboelectric nanogenerators, *Nano Energy* 81 (2021), 105627, <https://doi.org/10.1016/j.nanoen.2020.105627>.
- [16] L.Y.Z. Shuai, Z.H. Guo, P.P. Zhang, J.M. Wan, X. Pu, Z.L. Wang, Stretchable, self-healing, conductive hydrogel fibers for strain sensing and triboelectric energy-harvesting smart textiles, *Nano Energy* 78 (2020), 105389, <https://doi.org/10.1016/j.nanoen.2020.105389>.
- [17] S.S. Kwak, H.J. Yoon, S.W. Kim, Textile-based triboelectric nanogenerators for self-powered wearable electronics, *Adv. Funct. Mater.* 29 (2019), 1804533, <https://doi.org/10.1002/adfm.201804533>.
- [18] S.S. Kwak, H. Kim, W. Seung, J. Kim, R. Hinchet, S.W. Kim, Fully stretchable textile triboelectric nanogenerator with knitted fabric structures, *ACS Nano* 11 (2017) 10733–10741, <https://doi.org/10.1021/acsnano.7b05203>.
- [19] Z. Zhou, K. Chen, X. Li, S. Zhang, Y. Wu, Y. Zhou, K. Meng, C. Sun, Q. He, W. Fan, E. Fan, Z. Lin, X. Tan, W. Deng, J. Yang, J. Chen, Sign-to-speech translation using machine-learning-assisted stretchable sensor arrays, *Nat. Electron.* 3 (2020) 571–578, <https://doi.org/10.1038/s41928-020-0428-6>.
- [20] Z.L. Wang, Triboelectric nanogenerators as new energy technology and self-powered sensors - principles, problems and perspectives, *Faraday Discuss.* 176 (2014) 447–458, <https://doi.org/10.1039/c4fd00159a>.
- [21] Z.L. Wang, J. Chen, L. Lin, Progress in triboelectric nanogenerators as a new energy technology and self-powered sensors, *Energy Environ. Sci.* 8 (2015) 2250–2282, <https://doi.org/10.1039/c5ee01532d>.
- [22] C.S. Wu, A.C. Wang, W.B. Ding, H.Y. Guo, Z.L. Wang, Triboelectric nanogenerator: A foundation of the energy for the new era, *Adv. Energy Mater.* 9 (2019), 1802906, <https://doi.org/10.1002/aenm.201802906>.
- [23] Y. Zou, V. Raveendran, J. Chen, Wearable triboelectric nanogenerators for biomechanical energy harvesting, *Nano Energy* 77 (2020), 105303, <https://doi.org/10.1016/j.nanoen.2020.105303>.
- [24] W. Seung, H.J. Yoon, T.Y. Kim, M. Kang, J. Kim, H. Kim, S.M. Kim, S.W. Kim, Dual friction mode textile-based tire cord triboelectric nanogenerator, *Adv. Funct. Mater.* 30 (2020), 2002401, <https://doi.org/10.1002/adfm.202002401>.
- [25] Z. Li, M. Zhu, Q. Qiu, J. Yu, B. Ding, Multilayered fiber-based triboelectric nanogenerator with high performance for biomechanical energy harvesting, *Nano Energy* 53 (2018) 726–733, <https://doi.org/10.1016/j.nanoen.2018.09.039>.
- [26] X. Pu, W.X. Song, M.M. Liu, C.W. Sun, C.H. Du, C.Y. Jiang, X. Huang, D.C. Zou, W. G. Hu, Z.L. Wang, Wearable power-textiles by integrating fabric triboelectric nanogenerators and fiber-shaped dye-sensitized solar cells, *Adv. Energy Mater.* 6 (2016), 1601048, <https://doi.org/10.1002/aenm.201601048>.
- [27] X. Pu, L. Li, M. Liu, C. Jiang, C. Du, Z. Zhao, W. Hu, Z.L. Wang, Wearable self-charging power textile based on flexible yarn supercapacitors and fabric nanogenerators, *Adv. Mater.* 28 (2016) 98–105, <https://doi.org/10.1002/adma.201504403>.
- [28] Z. Cong, W. Guo, Z. Guo, Y. Chen, M. Liu, T. Hou, X. Pu, W. Hu, Z.L. Wang, Stretchable coplanar self-charging power textile with resist-dyeing triboelectric nanogenerators and microsupercapacitors, *ACS Nano* 14 (2020) 5590–5599, <https://doi.org/10.1021/acsnano.9b09994>.
- [29] C.Y. Chen, L.J. Chen, Z.Y. Wu, H.Y. Guo, W.D. Yu, Z.Q. Du, Z.L. Wang, 3d double-faced interlock fabric triboelectric nanogenerator for bio-motion energy harvesting and as self-powered stretching and 3d tactile sensors, *Mater. Today* 32 (2020) 84–93, <https://doi.org/10.1016/j.mattod.2019.10.025>.
- [30] M.M. Liu, Z.F. Cong, X. Pu, W.B. Guo, T. Liu, M. Li, Y. Zhang, W.G. Hu, Z.L. Wang, High-energy asymmetric supercapacitor yarns for self-charging power textiles, *Adv. Funct. Mater.* 29 (2019), 1806298, <https://doi.org/10.1002/adfm.201806298>.
- [31] L. Ma, M. Zhou, R. Wu, A. Patil, H. Gong, S. Zhu, T. Wang, Y. Zhang, S. Shen, K. Dong, L. Yang, J. Wang, W. Guo, Z.L. Wang, Continuous and scalable manufacture of hybridized nano-micro triboelectric yarns for energy harvesting and signal sensing, *ACS Nano* 14 (2020) 4716–4726, <https://doi.org/10.1021/acsnano.0c00524>.
- [32] Q. Qiu, M.M. Zhu, Z.L. Li, K.L. Qiu, X.Y. Liu, J.Y. Yu, B. Ding, Highly flexible, breathable, tailorable and washable power generation fabrics for wearable electronics, *Nano Energy* 58 (2019) 750–758, <https://doi.org/10.1016/j.nanoen.2019.02.010>.
- [33] Z. Li, M. Zhu, J. Shen, Q. Qiu, J. Yu, B. Ding, All-fiber structured electronic skin with high elasticity and breathability, *Adv. Funct. Mater.* 30 (2019), 1908411, <https://doi.org/10.1002/adfm.201908411>.
- [34] Y.D. Li, Y.N. Li, M. Su, W.B. Li, Y.F. Li, H.Z. Li, X. Qian, X.Y. Zhang, F.Y. Li, Y. L. Song, Electronic textile by dyeing method for multiresolution physical kineses monitoring, *Adv. Electron. Mater.* 3 (2017), 1700253, <https://doi.org/10.1002/aeml.201700253>.
- [35] H. Li, S.Y. Zhao, X.Y. Du, J.N. Wang, R. Cao, Y. Xing, C.J. Li, A compound yarn based wearable triboelectric nanogenerator for self-powered wearable electronics, *Adv. Mater. Technol.* 3 (2018), 1800065, <https://doi.org/10.1002/admt.201800065>.

- [36] A. Yu, X. Pu, R. Wen, M. Liu, T. Zhou, K. Zhang, Y. Zhang, J. Zhai, W. Hu, Z. L. Wang, Core-shell-yarn-based triboelectric nanogenerator textiles as power cloths, *ACS Nano* 11 (2017) 12764–12771, <https://doi.org/10.1021/acsnano.7b07534>.
- [37] W. Fan, Q. He, K. Meng, X. Tan, Z. Zhou, G. Zhang, J. Yang, Z.L. Wang, Machine-knitted washable sensor array textile for precise epidermal physiological signal monitoring, *Sci. Adv.* 6 (2020) 2840, <https://doi.org/10.1126/sciadv.aay2840>.
- [38] F. Xi, Y. Pang, W. Li, T. Jiang, L. Zhang, T. Guo, G. Liu, C. Zhang, Z.L. Wang, Universal power management strategy for triboelectric nanogenerator, *Nano Energy* 37 (2017) 168–176, <https://doi.org/10.1016/j.nanoen.2017.05.027>.
- [39] X. Liang, T. Jiang, G. Liu, Y. Feng, C. Zhang, Z.L. Wang, Spherical triboelectric nanogenerator integrated with power management module for harvesting multidirectional water wave energy, *Energy Environ. Sci.* 13 (2020) 277–285, <https://doi.org/10.1039/c9ee03258d>.
- [40] W. Yang, W. Gong, C. Hou, Y. Su, Y. Guo, W. Zhang, Y. Li, Q. Zhang, H. Wang, All-fiber tribo-ferroelectric synergistic electronics with high thermal-moisture stability and comfortability, *Nat. Commun.* 10 (2019) 5541, <https://doi.org/10.1038/s41467-019-13569-5>.
- [41] X. Cheng, W. Tang, Y. Song, H. Chen, H. Zhang, Z.L. Wang, Power management and effective energy storage of pulsed output from triboelectric nanogenerator, *Nano Energy* 61 (2019) 517–532, <https://doi.org/10.1016/j.nanoen.2019.04.096>.
- [42] W. Harmon, D. Bamgboje, H.Y. Guo, T.S. Hu, Z.L. Wang, Self-driven power management system for triboelectric nanogenerators, *Nano Energy* 71 (2020), 104642, <https://doi.org/10.1016/j.nanoen.2020.104642>.
- [43] H.F. Qin, G.Q. Gu, W.Y. Shang, H.C. Luo, W.H. Zhang, P. Cui, B. Zhang, J.M. Guo, G. Cheng, Z.L. Du, A universal and passive power management circuit with high efficiency for pulsed triboelectric nanogenerator, *Nano Energy* 68 (2020), 104372, <https://doi.org/10.1016/j.nanoen.2019.104372>.



Chongxiang Pan received his M.S. degree from Department of Materials Science and Engineering, Shenyang University of Chemical Technology in 2019. He is now pursuing his Ph. D. degree at Guangxi University. His research interests focus on the energy harvesting materials and devices.



Zi Hao Guo received his postgraduate degree in Materials Engineering from University of science and technology of Beijing. Now he is pursuing his doctor's degree in Beijing Institute of Nanoenergy and Nanosystem, Chinese Academy of Sciences. His current research mainly focuses on flexible self-charging systems and human-machine interaction systems.



Wenbin Guo received his M.S. degree from Department of Chemistry, Capital Normal University in 2018, he is currently pursuing his Ph.D. degree at Beijing Institute of Nanoenergy and Nanosystems, CAS. His research is focused on the Zn-ion battery.



Longwei Li received his B.S and M.S degree from the Department of Polymer Materials Science and Engineering, Dalian University of Technology in 2017 and 2020, respectively. Now he is pursuing his Doctoral degree at Beijing Institute of Nanoenergy and Nanosystem, CAS. His research interests mainly focus on ionic electronics energy and sensor devices.



Prof. Yanping Liu is an associate professor from College of Textiles at Donghua University. He received his Ph.D. degree from the Hong Kong Polytechnic University in 2013. His research focuses on knitting technology, 3D knitted products, and smart electronic textiles. He has published more than 30 peer-reviewed journal articles, and four chapters in related areas.



Fan Xu received her B.S. degree from Department of Materials Science and Engineering, University of Shanghai for Science and Technology in 2014. Now pursuing her Ph.D. degree at Beijing Institute of Nanoenergy and Nanosystems, CAS. Her research interests focus on smart electronic textiles, wearable functional electronics.



Shanshan Dong received her M.S. degree in Textile Engineering from Donghua University in 2020. Her research interests include knitting technology and textile-based triboelectric nanogenerator for wearable electronics.



Guoxu Liu received his Ph.D. degree from University of Chinese Academy of Sciences (National Center for Nanoscience) in 2021. Now he is doing postdoctoral research at Shenzhen University, and as a visiting scholar in Beijing Institute of Nanoenergy and Nanosystems, Chinese Academic Science. His current research mainly focuses on energy harvesting and fabrication of nanodevices.



Prof. Chi Zhang received his Ph.D. degree from Tsinghua University in 2009. After graduation, he worked in Tsinghua University as a postdoc research fellow and NSK Ltd., Japan as a visiting scholar. He now is the principal investigator of Tribotronics Group in Beijing Institute of Nanoenergy and Nanosystems, Chinese Academy of Sciences. Prof. Chi Zhang's research interests are triboelectric nanogenerator, tribotronics, self-powered MEMS/ NEMS, and applications in flexible electronics, intelligent equipment and the Internet of things. He has been awarded the National Science Fund for Excellent Young Scholars.



Prof. Zhong Lin Wang is the Chief scientist and Director of Beijing Institute of Nanoenergy and Nanosystems, Chinese Academy of Sciences. He is also the Regents' Professor and Engineering Distinguished Professor at Georgia Institute of Technology. His discovery and breakthroughs in developing nanogenerators establish the principle and technological road map for harvesting mechanical energy from environmental for powering personal electronics. He coined and pioneered the field of piezotronics and piezo-phototronics by introducing piezoelectric potential-gated charge transport process in fabricating new electronic and optoelectronic devices. Details can be found at: <http://www.nanoscience.gatech.edu>.



Prof. Xiong Pu is an associate professor and principle investigator at Beijing Institute of Nanoenergy and Nanosystems (BINN), Chinese Academy of Sciences. He received his Ph.D. degree from Department of Materials Science and Engineering of Texas A&M University in 2014. His research focuses on the energy harvesting materials and devices, triboelectric nanogenerators, self-charging power systems, and smart electronic textiles. He has published more than 50 peer-reviewed journal articles, and two chapters in related areas.